Effects of the Bonding Temperature and Annealing towards the Micro-structural of Thermosonic Cu-Al Interface

T. J. S. Anand[a,*], K.Y. Chua[b], S. Shariza[a], C.C. Lee[b] , D. Ranjith Kumar[c]

[a] Advanced Manufacturing Centre, Fakulti Kejuruterran Pembuatan, Universiti Teknikal Malaysia Melaka, Hang Tuah Jaya, 76100 Durian Tunggal, Melaka, Malaysia.

[b] Infineon Technology (Malaysia) Sdn. Bhd., FTZ Batu Berendam, 75350 Melaka Malaysia.

[c] Department of Nanoscience and Technology, Bhrathiar University, Coimbatore-641046, India.

*corresponding author: anand@utem.edu.my

Abstract: In this study, effects of bonding temperature and annealing towards the micro-structural evolution of the IMC at the bonding interface were evaluated. Analyses using Scanning Transmission Electron Microscope equipped with Energy Dispersive X-ray facility were performed. It was observed that an increased bonding temperature resulted in a rapid interdiffusion of Cu-Al in as-synthesized sample. A higher bonding temperature resulted in a thicker and more uniform IMC formation at the bonding interface. Grain boundary diffusion was prominent at the bonding temperature of 100°C; while volume diffusion was dominated at 280 and 400°C. An exponential relationship between total IMC thickness and bonding temperature was observed. After 1000 hours of annealing / HTS treatment, a depletion of the Al bond pad and diffusion of Cu into Si to form precipitates were observed. The chemical analysis revealed that multiple phases co-existed at the bonding interface especially for the sample synthesized with a lower bonding temperature. Moreover, the IMC layer with a superlattice-like structure was observed in the annealed sample synthesized with higher bonding temperature. This observation did not suggest a volume diffusion mechanism for the growth of the IMC layer. The reason for this kind of diffusion behaviour will need further investigations.

Keywords: Intermetallic Compounds; Wire bonding; Scanning Transmission Electron Microscope; Grain Boundary diffusion

1. INTRODUCTION

Thermosonic wire bonding is a common method for interconnection application in micro-electronic packaging industry [1]. Incorporation of ultrasonic, thermal energies as well as mechanical compression forces achieve the welding between wire and bond pad materials [2,3].

Gold (Au) wire was traditionally used as the interconnection material between bond pad and leadframe or substrate. Au wire material possesses beneficial characteristics, i.e. soft in nature and never oxidizes in ambient. These material properties make Au wire to facilitate a productive wire bonding process. However, an alternative material for replacing expensive Au wire is required for reducing the cost of production. It is highlighted that some high pin count and fine pitch packages may requires total wire length more than 5m. Therefore, a replacement of Au wire with other low cost material means a significant cost saving in production [4]. Various potential wire materials have been assessed, e.g. Copper (Cu), Palladium (Pd), Al (Aluminum) and Silver (Ag). Among these materials, Cu is the most promising material in term of the interconnection reliability [2]. As compare to Au, Cu owns material properties of higher / better electrical and thermal conductivities [5] that are suitable for high power and high speed functionality. Moreover, a relatively higher Elastic Modulus helps in

minimizing the sagging wire during the mould encapsulation process [4].

In micro-electronic packaging industry, Aluminum (Al) bond pad has been dominant for interconnection application. It serves as the Input/Output terminal that links to external circuit through bonded wires. A combination of Cu wire and Al bond pad has been extensively studied [3,6,7]. A high importance is given to morphological and chemical analysis of the intermetallic compound (IMC) developed at the bonding interface after annealing [8–10]. The annealing condition for Thermosonic Cu-Al system is usually referring to High Temperature Storage (HTS). HTS is a standard annealing or aging process with typical temperature of 175°C for evaluating the long term reliability performance of the component in micro-electronics industry [11]. The IMC formation at the bonding interface is commonly believed to correlate to the reliability of the bonding and thus that of the electronic devices. General speaking, a sufficient growth of the IMC under a HTS condition enhances the bondability. However, an excessive growth of the IMC could lead to a degradation of reliability of the bonding due to the formation of voids and increase of electrical resistance [10,12,13]. The void formation is usually visible in the bonding interface of Cu-Al after annealing. The void formation is believed to originate from a volumetric shrinkage due to a phase transformation [14].

The bonding temperature is one of the key parameters that influence the micro-structure of the bonding interface and its bondability. It is highlighted that the Cu wire bonding temperature of 175°C enhances the fragmentation of native oxide on the Al bond pad surface. This facilitates the growth of the interfacial IMC by an enhanced interdiffusion [15]. Moreover, works of Murali et al [2] shows that the wire bonding at 200°C brings advantages of a softening of materials which eases the plastic deformation, surface oxides fracture, enhanced interdiffusion at bonding interface and supply of supplementary energy to aid wire bonding process. Nevertheless, it is noticed that the reported Cu wire bonding temperature is in the range of 25 to 220°C [15–17]. The research on the Cu wire bonding interface synthesized at a bonding temperature more than 220°C is uncommon. A higher bonding temperature could theoretically enhance the bonding if the interfacial IMC is sufficiently grown. On the other hand, the IMC thickness could be excessively grown and results in degradation of the bonding quality. Therefore, it is of scientific interest to understand the micro-structural evolution of the interfacial IMC at a higher bonding temperature. Anand et al [9] reported a FESEM EDX structural analysis of Cu-Al interface which was synthesized at the bonding temperature of 400°C after 500 hours of HTS treatment. It was observed that the higher bonding temperature induces a rapid interdiffusion and leads to the formation of Cu-rich IMC. However, the structural and chemical analyses in their works were restricted by the resolution of characterization methods and no comparison to as-synthesized sample.

The present research group reported a microstructural analysis of Thermosonic Cu wire-Al bond pad synthesized at 280°C [3]. However, the location studied was at the centre of the ball bond. This region is not equivalent to the high stress region where the Al bond pad is severely thinned due to stress concentration during the wire bonding process [3]. This high stress region is usually observed at the periphery of the ball bond and related to the initiation of void formation [10] and thus the reliability of the bonding. Therefore, micro-structures at a high stress region of the Cu-Al bonding interface that is synthesized at an elevated bonding temperature worth an in-depth study. Besides, micro-structural study by Tan et al [18] hints a different IMC growth kinetics in both central and peripheral regions of the bonding interface. Furthermore, there is limited

information on the effect of annealing towards the micro-structural evolution of the bonding interface of a batch of samples synthesized at various bonding temperatures.

In this work, effects of bonding temperatures and annealing toward the Cu-Al bonding interface at high stress region were studied. The formal analysis was carried out with samples synthesized at bonding temperatures of 100, 280 and 400°C. The latter analysis was performed with annealed samples that were initially synthesized at 100 and 280°C.

2. Experimental Procedure

Procedures for synthesizing the sample involved a eutectic die bonding which transfer micro-chips from a wafer to the leadframe. The die bonder used was TOSOK DBD1000. Then Thermosonic Cu wire bonding was performed using Shinkawa ACB35 at bonding temperatures of 100, 280 and 400°C. This wire bonder is capable to generate an ultrasonic vibration at 60kHz. Constance wire bonding parameters were: Ultrasonic power 30units, bond force 30g and bond time 15ms. Cu Free-Air-Ball size of about 55μm was generated by Electro-Flame-Off (EFO) feature of the wire bonder. Then selected samples were loaded into High Temperature Storage (HTS) chamber (ESPEC, PHH-201M) at 175°C for 1000 hours. After that samples were further prepared with the mechanical cross-section prior to focus ion beam (FIB) (FEI Nova Lab 200). In FIB, a thin lamella with dimension 10μm x 10μm x 0.1μm was extracted from the peripheral bonding interface (high stress region) consisting Si, Al bond pad and Cu ball bond. Equipment and process parameters used in these processes were similar to that of [3,11], except that the bonding temperatures evaluated in this work were 100, 280 and 400°C. Moreover, selected samples for annealing were that synthesized with bonding temperature of 100 and 280°C. Lamellas were then inspected by FEI TECNAI G2F20 system which is capable for Scanning TEM (STEM) imaging with high angle annular dark field (HAADF) feature and line scan Energy Dispersive X-ray (EDX).

3. Results and Discussion

3.1 Effects of Thermosonic bonding temperatures

Figure 1 shows the STEM results for sample synthesized at bonding temperature of 100°C. From Figure 1a, it was observed that the Al bond pad experienced a severe thinning (from the original thickness of 1μm to as thin as 0.4μm) after Thermosonic wire bonding process. The severe Al thinning is an indication of the high stress region. This is explained through the maximum stress generated only in the periphery of the bonding interface due to the geometry of the capillary [19]. This high stress in turn results in severe deformation and "squeeze out" of Al bond pad in the periphery [10]. On the other hand, central region of the as-synthesized bonding interface is with a relatively thicker Al thickness. This is due to the "squeeze out" of Al in the periphery that transfers some amount of Al to the central region of the bonding interface [10]. Besides, a gap between Cu and Si was visible in the top portion of the lamella. This gap is originated from the absence of Al due to "squeeze out" of Al during ultrasonic scrubbing under compression pressure [2]. Furthermore, there was hardly found any obvious intermetallic compound (IMC) at the Cu-Al bonding interface from overview STEM image in Figure 1a. Instead some grains were observed within the Al bond pad as shown in the magnified STEM image in Figure 1b. Figure 1c was a magnified STEM micrograph where a thin layer of IMC was possibly existed at the bonding interface. The confirmation and identification of the intermetallic phase was achieved by first measuring the composition (EDX line scan) along the suspected region (red arrows in Figure 1b and c). Compositional information obtained was then

referring to the Cu-Al binary phase diagram [20] for phase identification.

Figure 2a and b were compositional analysis results of line scans as defined by arrows i and ii in Figure 1b, respectively. These regions consisted of 2 visible grains within the Al bond pad (see Figure 1.b). Shaded area in the graphs represents the possible location of IMC. The corresponding phase within the shaded areas was a mixture of α-Al + $CuAl_2$. The estimated mass fraction ratio of α-Al: $CuAl_2$ was calculated based on the average value of the composition. The mass fraction ratio of α-Al:$CuAl_2$ for Figure 2a and b were 0.11:0.89 and 0.68:0.32, respectively. A significant variation in mass fraction of phases of these grains in a localized region showed a low uniformity in the chemical distribution. Moreover, the formation of IMC grains without in contact with the Cu ball bond implied that the IMC formation was by grain boundary diffusion mechanism.

Figure 2c and d show the line scan EDX results defined in Figure 1c, i.e. arrows iii and iv, respectively. These measurements were performed across the thin IMC layer at the Cu-Al bonding interface. From Figure 2c, it was observed that the IMC exist from the starting point until about 20nm along the scanning line. The IMC was formed at the bond pad side. From the composition profile, the IMC observed was a mixture of α-Al + $CuAl_2$ phases. A transition with thickness of about 20nm where both Cu and Al interdiffused was observed next to the IMC. Figure 2d shows a similar observation, i.e. a 35nm thick layer of mixture of α-Al + $CuAl_2$ phases formed at the bond pad side and a thin transition region (~25nm) was observed next to the IMC formed. The estimated mass fraction ratio of α-Al: $CuAl_2$ for both Figure 2c and d were 0.57:0.43 and 0.68:0.32, respectively. With the suggestion of micro-structure of sputtered Cu-Al film [21], the $CuAl_2$ phase was expected to be the major precipitated component in the α-Al matrix. These IMC that were in layered form and connected to Cu ball bond were grown by volume diffusion mechanism as commonly observed by others [12,22].

Figure 3 shows the STEM imaging results for the lamella extracted from the sample synthesized at bonding temperature of 280°C. It was obviously seen that there was a gap at the bonding interface as seen in the middle portion of Figure 3a. This region did not form an IMC and belonged to an unbounded region which originates from non-uniform ultrasonic energy transfer from capillary to the bond pad [3,23]. This statement was supported by the following compositional analysis along a scan line crossing the unbounded region at the bonding interface (arrow i in Figure 3b). The region consisted of the gap had an Al bond pad thickness of about 500nm which was thicker than that of the bottom portion of the lamella in Figure 3a. Therefore, the bottom portion of the lamella was corresponded to the high stress region. Furthermore, an obvious layer of IMC was observed at the bonding interface at the bottom portion of the lamella. This again indicated that this area was in a higher stress condition that generated a higher interfacial temperature and in turn promoted the IMC growth. This is evident through the works of Tan et al [18] that performed STEM micro-structural analysis at the Thermosonic bonding interface of Cu wired Al bond pad. From their inspection results on as-synthesized sample, the IMC formation at the centre of the ball bond is inhomogeneous and thinner compared to that of the periphery (high stress region). Figure 3b and c revealed the existence of IMC layers with thicknesses of ~35nm and 75nm, respectively, at the bonding interface. An inset of Figure 3c shows the magnified STEM image which focuses on the Al bond pad with a formation of particles. The following compositional analysis suggested that the particles were the precipitation of Cu.

Figure 4a to d show results of the compositional analysis by line scan EDX for arrows i to iv defined

in Figure 3b and c. Figure 4a shows the result which focussed at the gap at the bonding interface. It shows that the interdiffusion of both Cu and Al occurred though the gap existed. This indicated that the Cu ball bond and Al bond pad were initially in contact. However, the bonding was not successful. Moreover, it was observed that the content of Oxygen (O) element rose to about 20wt% for the portion near the bonding interface especially at the Al side. This indicated the existence of Alumina. Figure 4b shows the line scan EDX result crossing an obvious darker layer by the gap at the bonding interface (defined as arrow ii in Figure 3b). It was seen that the darker layer consisted of O, especially at the close to the boundaries of Cu and Al. This indicated an ineffective ultrasonic scrubbing of oxides during Thermosonic wire bonding process. As the composition profile of O varied with that of Al, it suggested that this darker layer was corresponded to Alumina. From both Figure 4a and b, Alumina layer did not impede the interdiffusion of Cu and Al. Similar comments are given by Xu et al [14] who observe the formation of Cu_9Al_4 phase around Alumina after annealing and Funamizu et al [24] who use Alumina as markers for Cu-Al interdiffusion couple. Figure 4c shows the line scan result across an IMC layer formed at the bonding interface (arrow iii in Figure 3b). From the compositional analysis, the IMC layer consisted of a mixture of α-Al + $CuAl_2$ phases with a mass fraction ratio of α-Al:$CuAl_2$ = 0.07:0.93. Figure 4d is the line scan result across the IMC layer located at the bonding interface in the high stress region (arrow iv in Figure 3c). The corresponding phases were mixtures of $CuAl_2$ + CuAl with mass fraction ratio of $CuAl_2$:CuAl = 0.75:0.25. The formation of this IMC with a higher Cu mass fraction indicated a more rapid interdiffusion in high stress region. This was in a good agreement with the empirical observation by Tan et al [18].

Moreover, the measurement along the arrow iv did cross a few particles present within the Al bond pad as labelled in Figure 4d. A slight increase of Cu contents (<4wt%) of the particles indicated a mixture of α-Al + CuAl2 phase with a high mass fraction of Al (>0.93). The origin of the formation of particles was explained through a temperature fall from that above the solvus line (≥500°C for 4wt% Cu) according to the Cu-Al binary phase diagram. When the temperature decreased below the solvus line, the solubility of Cu in Al was exceeded and in turn resulted in precipitation of Cu particle in Al. A similar mechanism is given in [5] for eutectic Cu-tin (Sn) alloy. According to Anand et al [3], the temperature could rise up to 437°C at the center region of a ball bond though the wire bonding process is performed at only 280°C. The interfacial temperature was predicted from the single phase IMC thickness measurement and the IMC growth kinetics in Arrhenius relation [24]. It was reasonably believed that a temperature > 500°C could be achieved at the high stress region of sample synthesized at 280°C.

Figure 5 shows the STEM imaging result for the sample prepared with bonding temperature of 400°C. Figure 5a is the overview image of the lamella. It was observed that the remnant of the Al bond pad was with the thickness of ~100nm. This indicated a severe Al thinning and thus the high stress area was included in the lamella. Besides, a localized region without a visually obvious IMC formation was seen in the middle portion of the lamella. In fact, from the composition analysis in this region, as discussed in a later section, the Cu-Al interdiffusion did occur. This localized region was where an ultrasonic energy was transferred ineffectively from the vibrating capillary to the bonding interface [25] and in turn caused a lower interfacial temperature. Therefore, a poorer interdiffusion occurred in this region. Furthermore, a relatively thick and homogenous IMC formation could be observed at the bonding interface, except near the middle portion of the lamella. The IMC layer could be seen obviously in magnified images of STEM in Figure 5b and c. The

estimated IMC thickness was about 160nm. It was observed that the IMC thickness in both top (Figure 5b) and bottom (Figure 5c) portions of the lamella were not statistically different, after a t-test was carried out to compare the mean of thicknesses from both locations.

Figure 6 shows the line scan EDX results for arrows defined in Figure 5. These measurements crossed the IMC layer that formed at the bonding interface. Figure 6a shows that two layers of IMC were present with different thickness and composition at the bonding interface in the middle portion of the lamella (arrow i). The thicker IMC layer in the left of Figure 6a (termed as A) and the other thinner IMC layer (termed as B) had a thickness of ~170 and 20nm, respectively. From the compositional analysis, both IMC layers were mixtures of α-Al + CuAl2 phases. The mass fraction ratio of α-Al:CuAl2 are 0.90:0.10 and 0.02:0.98 for IMC A and IMC B, respectively. Therefore the interdiffusion did occur and resulted in the formation of the IMC in this region though the IMC was not obviously seen in the STEM image (Figure 5a). Figure 6b and c show the line scan EDX results crossed the bonding interface along the arrows ii and iii as defined in Figure 5b and c. From Figure 6b, a IMC layer with thickness about 80nm consisted of a mixture of α2 + Cu9Al4 was observed. Figure 6c shows that a 140nm thick IMC layer consisted of a similar α2 + Cu9Al4 phases were present at the bonding interface. The mass fraction ratio of α2:Cu9Al4 for both IMC layer as observed in Figure 6b and c were 0.89:0.11 and 0.46:0.54, respectively. The increment of the Al content of the IMC layer observed in the bottom portion of the lamella (Figure 5) was due to an enhanced interdiffusion at the high stress region.

From results of both imaging and compositional analyses, it had been generally observed that the thickness of the IMC formation (excluded IMC grains) at the as-synthesized bonding interface increased proportionally with bonding temperatures. These thicknesses were referring to the IMC formation connected to Cu and formed by common volume diffusion mechanism. A higher bonding temperature resulted in a thicker the IMC formation. This was expected as generally the rate of solid state reaction increases with temperature. Figure 7a shows the plot of the IMC thickness measured from STEM images, i.e. Figure 1c, 2c and 3c with similar magnification around the high stress region. It seemed the IMC thickness increase with the bonding temperature in an exponential manner. This was further verified by analysing the linearity between ln(IMC thicknesses) and bonding temperatures by Least Square Method. Figure 7b shows the result of the regression analysis. A strong linear correlation between ln(IMC thicknesses) and bonding temperatures was upheld within the range of temperature evaluated. The coefficient of determination (R2 value) of 0.85 was obtained. An empirical equation that fit the measurement was generated, i.e.

$$IMC\ thickness, x = Ae^{BT} \qquad (1)$$

where A = 7.0414 (nm) and B = 0.0079°C^{-1}.

The relationship between IMC thickness and bonding temperature of as-synthesized bonding interface was a topic seldom studied by other researchers. Studies of annealed IMC in bulk [24] and Thermosonic bonding interface [12,22] show a well-known relationship between IMC thickness and annealing duration as follow:

$$W = k_0 e^{\left(-\frac{Q}{RT}\right)}\sqrt{t} \qquad (2)$$

Where k0 = IMC growth rate pre-factor (ms-1/2), Q = activation energy for IMC growth (Jmol-1), R = molar gas constant = 8.314 JK-1mol-1, T = annealing temperature (K) and t = annealing duration. Equation (2) shows an Arrhenius relationship between W and T, if t was a constant.

To apply equation (2) in the as-synthesized system, T was interpreted as bonding temperature and t was the bond time (15ms). These conditions theoretically supported the Arrhenius relationship between W and T. However, the IMC thickness-bonding temperature profile measured in this work (Figure 7) did not agree with Arrhenius relationship. The possible explanation of the difference in observed and expected behaviours was as follow: Equation (3) was an empirical conclusion based on annealed metal couples which were pre-welded or pre-bonded prior to annealing. This equation did not take IMC formation at pre-welding or pre-bonding stage into account. Instead it only focused on the IMC growth kinetics during annealing process. On the other hand, exponential relationship of IMC thickness and bonding temperature as obtained empirically in this work reflected the kinetics of IMC formation within a short bonding time. Thermosonic wire bonding in the as-synthesized stage involved two processes before a successful ball bond is made, i.e. oxides/contamination fragmentation and solid state welding/bonding by interdiffusion [15]. Each of these processes occupied some split of t (say t_f and t_w for fragmentation time and welding time, respectively) and these processes to be completed within the bond time set, t ($t = t_f + t_w$). t_w was the time component contributed to the actual bonding. It is known that a higher bonding temperature softens the surface oxide/contamination layers that eases the fragmentation process [2]. Therefore it was expected that the time required for this fragmentation at a higher temperature was shorter than a low temperature did. In other words, the time allocation for solid state welding (t_w) increased when a higher bonding temperature was involved. Moreover, a higher bonding temperature that enhances the atomic diffusion of Cu and Al facilitating the thickening of the IMC layer [2,15] was another key factor for significant increment of IMC thickness at an elevated bonding temperature. A add-on effect of both increased duration of welding and enhanced atomic diffusion were believed attributed to the abrupt increase in IMC thickness in exponential manner at the elevated bonding temperature.

It was notice that the welding process within time interval of t_w was subjected to an effective interfacial temperature (T_e) that was resulted from both bonding temperature and temperature rise due to ultrasonic scrubbing. T_e in turn led to the interdiffusion of Cu and Al that caused the initial IMC formation at the bonding interface as observed in Figure 7 and Equation (1). One may assume that the initial IMC formation still comply with Equation (2) as the welding could be thought as an interdiffusion process at temperature T_e for a time duration of t_w. With this assumption, equation (1) and (2) could be re-written and equalized:

$$k'_0 e^{\left(-\frac{Q'}{RT_e}\right)}\sqrt{t_w} = Ae^{BT} \qquad (3)$$

Where k' = initial IMC growth rate pre-factor ($ms^{-1/2}$), Q = activation energy for initial IMC growth ($Jmol^{-1}$). There was no new definition for the rest of the variable and constant. Rearrangement of Equation (3) yielded:

$$T_e = \frac{Q'}{R\left[ln\left(\frac{k'_0\sqrt{t_w}}{A}-BT\right)\right]} \qquad (4)$$

Equation (4) demonstrated a reciprocal logarithm relationship of T_e and t_w. If T_e could be measured experimentally, e.g. to integrate a thin film thermal sensor under the bond pad to measure the interfacial temperature in situ [26], then the corresponded t_w could be estimated. However, equation (4) may be limited by little information with regard to as-synthesized IMC growth kinetics, e.g. k'0 and Q'.

Furthermore, it was observed that the IMC formation by grain boundary diffusion was dominated at the low bonding temperature of 100°C; while the higher bonding temperatures of 280 and 400°C facilitated the common IMC growth

by volume diffusion mechanism. Similar observation is observed and discussed by Harman for the diffusion of Cr into Au thin film [1]. Besides, a higher bonding temperature resulted in a more rapid Cu diffusion that caused a formation of phases with higher Cu content (CuAl and Cu9Al4 phases). The IMC formation with CuAl2 phase is commonly observed in as-synthesized samples [16,17] while CuAl and Cu9Al4 were usually observed annealed samples [12,22]. Researches on the effect of bonding temperature on the microstructure of the bonding interface were rare. This report could perhaps provide a better picture on how IMC thicknesses vary with bonding temperatures at as-synthesized state.

3.2 Effects of High Temperature Storage annealing

Figure 8 shows the STEM imaging results of the lamella extracted from the sample synthesized at the bonding temperature of 100°C and after HTS treatment. From Figure 8a, it was observed that Al had been fully consumed and turned into an IMC layer. This IMC layer was visually non-uniform in thickness. The estimated IMC thickness was 500nm. Figure 8b shows the magnified STEM image taken from the top portion of the lamella. It was observed that there was a formation of particles in Si (dark tone region). The chemical analysis was performed to study these particles. Besides, the IMC layer was apparently non-uniform in its image contrast. This observation indicated a non-uniform elemental distribution in the IMC layer as HAADF imaging contrast is dominated by atomic numbers of constituting atoms of the specimen [27]. Figure 8c was the magnified STEM image which focused in the middle portion of the lamella. A clearer boundary at the IMC-Si interface indicated that there was no major diffusion of Cu or Al into Si in this region. An analysis of the chemical distribution at the bonding interface was performed using line scan EDX measurement as defined arrows in Figure 8.

Figure 9a shows the line scan EDX result along the arrow i as defined in Figure 8b. There were two IMC layers observed and termed as C and D in the graph. C and D consisted of α_2 + Cu (mass fraction ratio α_2:Cu = 0.28:0.71) and Cu_9Al_4 + α_2 phases (mass fraction ratio Cu_9Al_4:α_2 = 0.60:0.40), respectively. Figure 9b shows another line scan EDX result at a location about 400nm away from arrow i in Figure 9a. The compositional profile revealed the formation of a distinctive IMC layer which consisted of Cu_4Al_3 + Cu_3Al_2 phases. The estimated mass fraction ratio of Cu_4Al_3:Cu_3Al_2 = 0.36:0.64. Figure 9c was the line scan result that measured across Cu, IMC layer and Si (see arrow iii defined in Figure 8c). It was observed that two IMC layers were formed, i.e. E and F as defined in Figure 9c. Predicted phase within these IMC layers were Cu_9Al_4 for E layer and mixture of $CuAl_2$ + CuAl for F layer, respectively. From above mentioned EDX results, a large variation in the chemical distribution at the bonding interface of this category of sample was observed. Moreover, from Figure 9a to c, a detection of Cu signal in Si region was observed. This indicated a diffusion of Cu atoms into Si. From the composition, the predicted phases were (Si) + η″- Cu_3Si [28,29]. η″ phase is phase with a orthorhombic structure and stable below 570°C [29]. On the other hand, diffusion of Al into Si was not prominent. This was explained from the aspect of activation energy. Chromik et al [28] summaries the activation energies of Cu diffusion in Si for forming Cu_3Si phase were in a range of 0.8 to 1.34eV. While from the report of Hwang et al [30], the activation energy for Al to diffuse in poly-silicon via grain boundary diffusion is 2.64eV. It is generally known that the activation energy of a volume diffusion event is greater than that of a grain boundary diffusion event. Therefore, the activation energy of Al atoms to diffuse in Si by volume diffusion was certainly higher than 2.64eV. Therefore, Al diffusion in Si was not observed in our study. A relatively high Cu content in Si region (see Figure 8a and b) resulted in a brighter tone in

STEM images (Figure 8b and c). This is again due to the atomic number dependence nature of HAADF imaging.

Figure 10 shows the STEM imaging result for the lamella extracted from the annealed sample synthesized at the bonding temperature of 280°C. From Figure 10a, two homogenous layers of IMC with uniform thickness were apparently formed at the bonding interface. A difference in the image contrast indicated a different composition distribution of each layer. The IMC layer which was close to Cu (darker tone) had an average thickness of about 250nm, while that of another layer (brighter tone) which was near to Si side was about 350nm. Figure 10b shows the magnified STEM image that focussed on the top portion of the lamella. It was observed that an additional IMC layer grew close to the Cu side (top portion of Figure 10b) with a thickness of ~90nm. Moreover, it was observed that there were particles in Si portion. Compositional analysis revealed that the diffusion of Cu into Si was the origin of this observation. Figure 10c shows an observation of particles formation within the IMC layer at the bonding interface. Similar compositional analysis was performed and discussed in the following section.

Figure 11 shows the line scan EDX results for scanning location as defined in Figure 10. Figure 11a shows the result of line scan that crossed the IMC layers formed at the top portion of the lamella (see Figure 10b). The line scan revealed that there were actually 3 layers of IMC. These IMC layers were termed as G, H and I in Figure 11a. Layers G and I were corresponded to $CuAl_2$ + CuAl. Layer I was corresponded to the mixture of α-Al + $CuAl_2$. Figure 11b was the line scan result at the bottom portion of Figure 10b. Three IMC layers were determined from the composition profile and termed as J, K and L in Figure 11b. Layers J and L were corresponded to α-Al + $CuAl_2$. Layer K was corresponded to the mixture of $CuAl_2$ + CuAl. From STEM image (Figure 10b), layers I, K and L were considered as an identical IMC layer. However, chemical compositions of these layers with 4 to 7wt% differences resulted in variations of phases. It was observed that the composition distribution of Cu decreased for a scanning distance and then increased again (see Figure 11a and b). This pattern of compositional distribution was uncommon. The most common compositional distribution at the bonding interface is that the content of an element gradually decreases with the scanning distance from its source [11,12,31]. The observed composition distribution of Cu resulted in a periodical structure of IMC layers or superlattice-like structure. The origin of the formation of this periodical structure was unknown and worth a future research. Furthermore, an obvious increase of Cu content in Si region was also seen in Figure 11b (distance = 0.89μm) that corresponded to a particle in Si. The compositions revealed that the particles found in Si were actually diffused Cu atoms that formed Cu_3Si phase.

Figure 11c presents the line scan result crossed a few particles within the IMC layer with brighter tones as seen in Figure 10a and c. It was observed that the IMC layer was a mixture of $CuAl_2$ + CuAl phases. The brighter particle in Figure 10c was actually a region where the content of Cu was slightly higher. Arrows in Figure 11c pointed out the locations of the particles. Formation of the particles could not be explained through the temperature falls below the solvus line as discussed in the previous section as annealing at 175°C did not supply of thermal energy to generate a temperature higher than ~590°C (solvus line for 60 wt% Cu). The possible explanation was that the particle was a nucleation site where the IMC continue to grow.

It was generally observed that the annealing at 175°C for 1000 hours had turned the Al bond pad into Cu-Al IMC. For sample synthesized at 100°C

and after HTS treatment, an irregular IMC formation was observed from STEM imaging and various intermetallic phases were detected within a localized region. This was potentially due to the simultaneous growth of IMC layers originated from grain boundary (refer Figure 1b) and volume diffusion (refer Figure 1c). For another sample synthesized at 280°C, uniform and homogenous IMC layers formed at the bonding interface as compared to that of sample synthesized at 100°C. However, the composition profile of Cu (superlattice-like structure) did not suggest the growth of the IMC was by common volume diffusion. The origin of this observation needs further studies.

4. Conclusion

In this work, effects of bonding temperature and HTS annealing had been evaluated on the Cu wired Al bond pad sample. STEM and line scan EDX analyses were the major tool in studying the morphology and composition of the IMC. At a lower bonding temperature (100°C), the IMC formation was inhomogeneous and dominated by grain boundary diffusion. At higher temperatures of 280 and 400°C, the thicker, more uniform and homogenous IMC formation by volume diffusion was observed. Besides, a higher bonding temperature resulted in a rapid Cu diffusion that leaded to a formation of higher Cu content phases (CuAl and Cu_9Al_4 phases). It was observed that an exponential relationship between IMC thickness and bonding temperature was observed instead of common Arrhenius relationship. A possible explanation was that the atomic diffusion and the welding duration increased with bonding temperature. After HTS annealing, it was generally observed that Al bond pad for samples synthesized at 100 and 280°C was fully consumed and turned into IMC layers. After annealing, the sample synthesized at a lower bonding temperature was observed to have irregular IMC layers with various phases at the bonding interface. Variation of phases existed in a localized region was believed due to the simultaneous growth of IMC originated from both grain boundary and volume diffusion. For another sample synthesized at higher bonding temperature, the annealing resulted in a formation of distinctive, uniform and homogenous IMC layers at the bonding interface. However, IMC layers showed a superlattice-like structure which may not suggest a volume diffusion mechanism. Further study on this observation is necessary. Furthermore, the Cu diffusion into Si was observed for both samples after annealing. This resulted in the formation of Cu_3Si particles within Si.

ACKNOWLEDGEMENTS

This study has been supported by Infineon (Melaka, Malaysia) Sdn. Bhd and Universiti Teknikal Malaysia Melaka (UTeM), Malaysia. The research work carried out under the collaborative research in engineering, Science and Technology (CREST) grant number GLuar/CREST/2015/FKP/I00004

REFERENCES

[1] Harman G. Wire Bonding in Microelectronics, 3rd ed. McGraw Hill Professional; 2010.

[2] Murali S, Srikanth N, Wong YM, Vath CJ. J Mater Sci 2006; 42:615.

[3] Anand TJS, Chua KY, Lim BH. Mater Chem Phys 2012; 136:638.

[4] Deley M, Levine L. The Emergence of High Volume Copper Ball Bonding, in: IEEE/CPMT/SEMI 29th Int. Electron. Manuf. Technol. Symp. (IEEE Cat. No.04CH37585). IEEE; 2004.

[5] Calister WD. Material Science and Engineering An Introduction, 6th ed. New York: John Wiley and Sons, Inc.; 2004.

[6] Onuki J, Koizumi M, Araki I. IEEE Trans Components, Hybrids, Manuf Technol 1987; 10:550.

[7] Qi J, Hung NC, Li M, Liu D. Scr Mater 2006; 54:293.

[8] Chen J, Lai Y-S, Wang Y-W, Kao CR. Microelectron Reliab 2011;51:125.

[9] Anand TJS, Yau CK, Leong YS, Keat LW, Ting HM. Curr Appl Phys 2013; 13:1674.

[10] Hang CJ, Wang CQ, Mayer M, Tian YH, Zhou Y, Wang HH. Microelectron Reliab 2008; 48:416.

[11] Chua KY, Hng MT, Lee CC, Anand TJS. Adv Mater Res 2012; 620:166.

[12] Xu H, Liu C, Silberschmidt V V., Chen Z. J Electron Mater 2009;39:124.

[13] Breach CD, Wulff FW. Microelectron Reliab 2010; 50:1.

[14] Xu H, Liu C, Silberschmidt VV, Pramana SS, White TJ, Chen Z, Acoff VL. Acta Mater 2011; 59:5661.

[15] Xu H, Liu C, Silberschmidt VV, Chen Z, Wei J, Sivakumar M. Microelectron Reliab 2011;51:113.

[16] Drozdov M, Gur G, Atzmon Z, Kaplan WD. J Mater Sci 2008; 43:6029.

[17] Xu H, Liu C, Silberschmidt VV, Pramana SS, White TJ, Chen Z. Scr Mater 2009; 61:165.

[18] Tan YY, Yong FK. Cu-Al IMC Micro Structure Study in Cu Wire Bonding with TEM, in: 2010 17th IEEE Int. Symp. Phys. Fail. Anal. Integr. Circuits. IEEE; 2010.

[19] Breach CD, Wulff F, Tok CW. Microelectron Reliab 2006; 46:543.

[20] Murray J. Int Met Rev 1985; 30.

[21] Idrac J, Blanc C, Kihn Y, Lafont MC, Mankowski G, Skeldon P, Thompson GE. J Electrochem Soc 2007; 154:C286.

[22] Kim H, Lee JY, Paik K, Koh K, Won J, Choe S, Lee J, Moon J, Park Y. IEEE Trans Components Packag Technol 2003;26:367.

[23] Wulff F, Breach C, Stephan D, Dittmer KJ. Characterisation of Intermetallic Growth in Copper and Gold Ball Bonds on Aluminium Metallization, in: Proc. 6th Electron. Packag. Technol. Conf. IEEE; 2004.

[24] Funamizu Y, Watanabe K. Trans Japan Inst Met 1971; 12:147.

[25] Hung L, Lin Y, Chen S, Wang Y, Hsiao CS. The Characterization of Intermetallic Growth in Copper and Gold Ball Bonded on Thicker Aluminum, in: 2006 7th Int. Conf. Electron. Packag. Technol. IEEE; 2006.

[26] Ho J, Chen C, Wang C. Sensors Actuators A Phys 2004; 111:188.

[27] Li K, Er E, Yeow T, Tang D. IEEE Trans Device Mater Reliab 2006;6:283.

[28] Chromik RR, Neils WK, Cotts EJ. J Appl Phys 1999; 86:4273.

[29] Olesinski RW, Abbaschian GJ. Bull Alloy Phase Diagrams 1986; 7:170.

[30] Hwang JC., Ho PS, Lewis JE, Campbell DR. J Appl Phys 1980; 51:1576.

[31] Li J, Han L, Duan J, Zhong J. Mater Charact 2007; 58:103.

Figure Captions

Fig. 1: STEM results for sample synthesized at bonding temperature of 100°C.

Fig 2: Compositional analysis results of line scans as defined by arrows i and ii in Figure 1b, respectively.

Fig. 3: STEM imaging results for the lamella extracted from the sample synthesized at bonding temperature of 280°C.

Fig. 4: Compositional analysis by line scan EDX for arrows i to iv defined in Figure 3b and c.

Fig. 5: STEM imaging result for the sample prepared with bonding temperature of 400°C

Figure 6: Compositional analysis by line scan EDX results for arrows defined in Figure 5

Figure 7: Compositional analysis by Plot of the IMC thickness measured from STEM images

Figure 8: STEM imaging results of the lamella extracted from the sample synthesized at the bonding temperature of 100°C.

Figure 9: Compositional analysis by line scan EDX result along the arrow i as defined in Figure 8.

Figure 10: STEM imaging result for the lamella extracted from the annealed sample synthesized at the bonding temperature of 280°C.

Figure 11: Compositional analysis by line scan EDX result along the arrow i as defined in Figure 10.

Figures

Figure 1

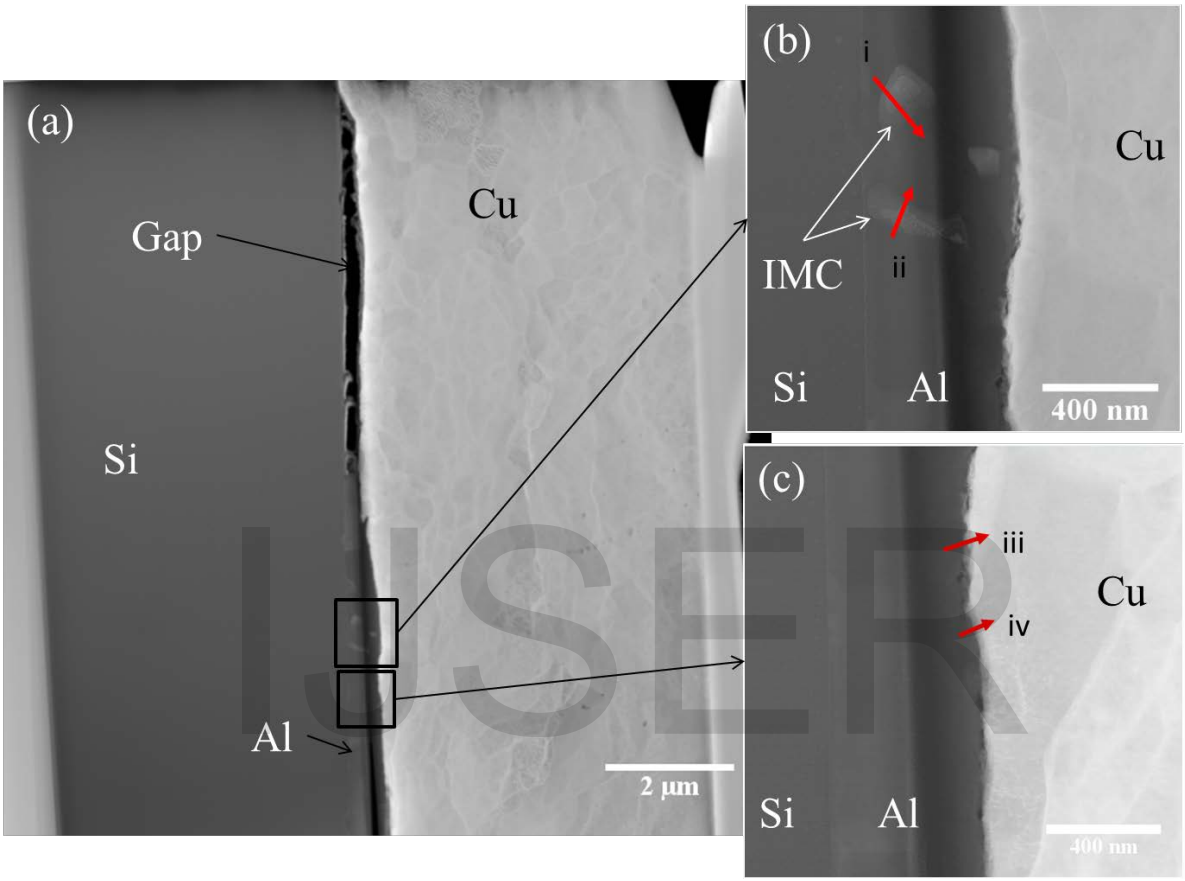

Figure 2

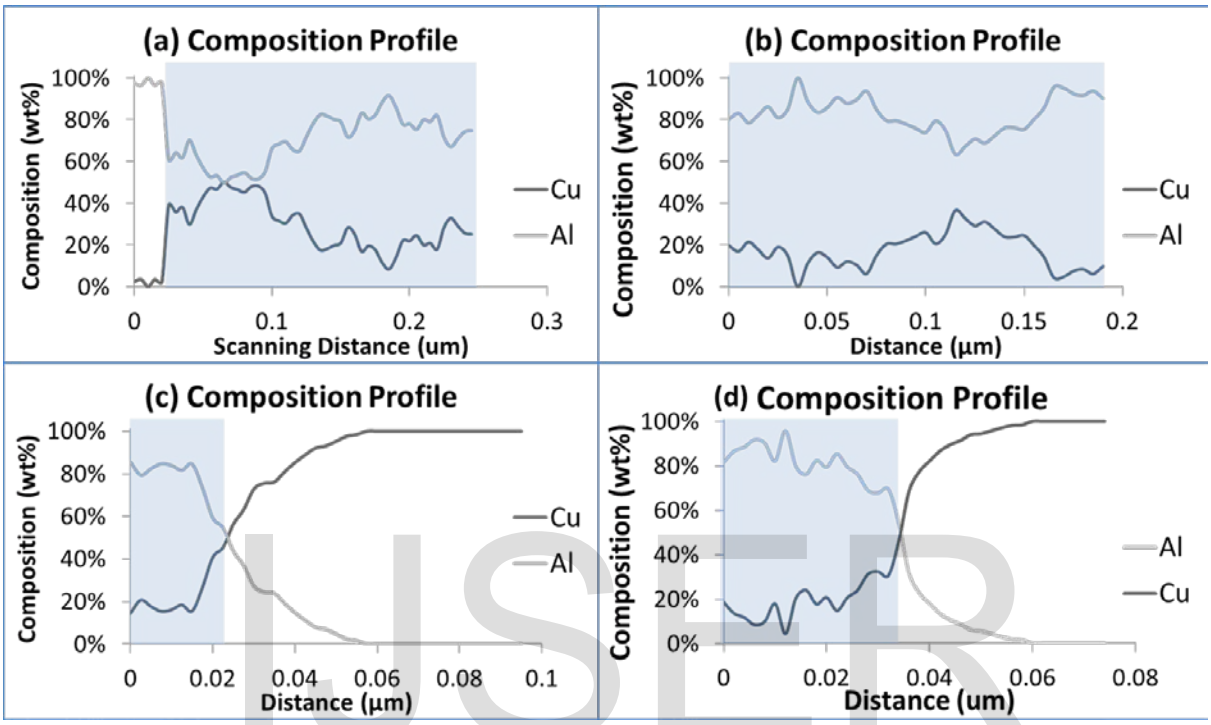

Figure 3

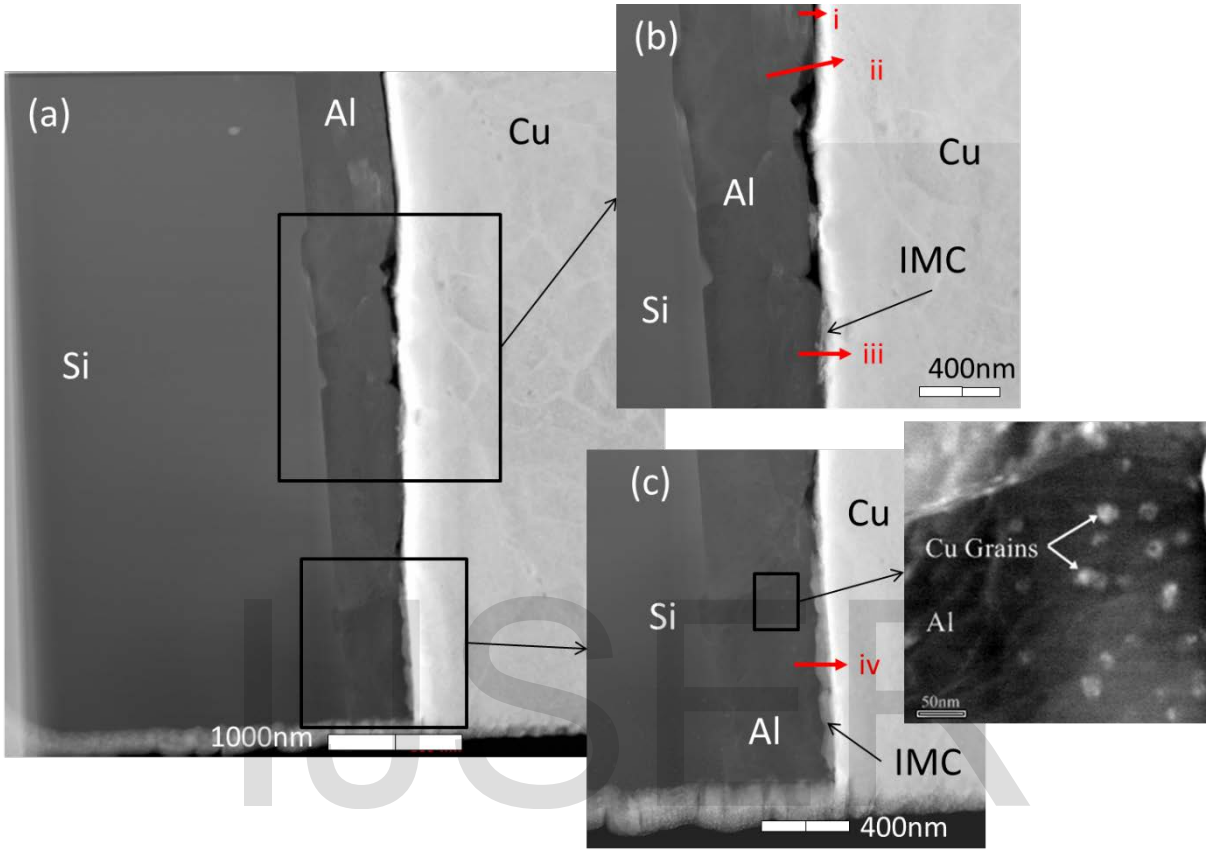

Figure 4

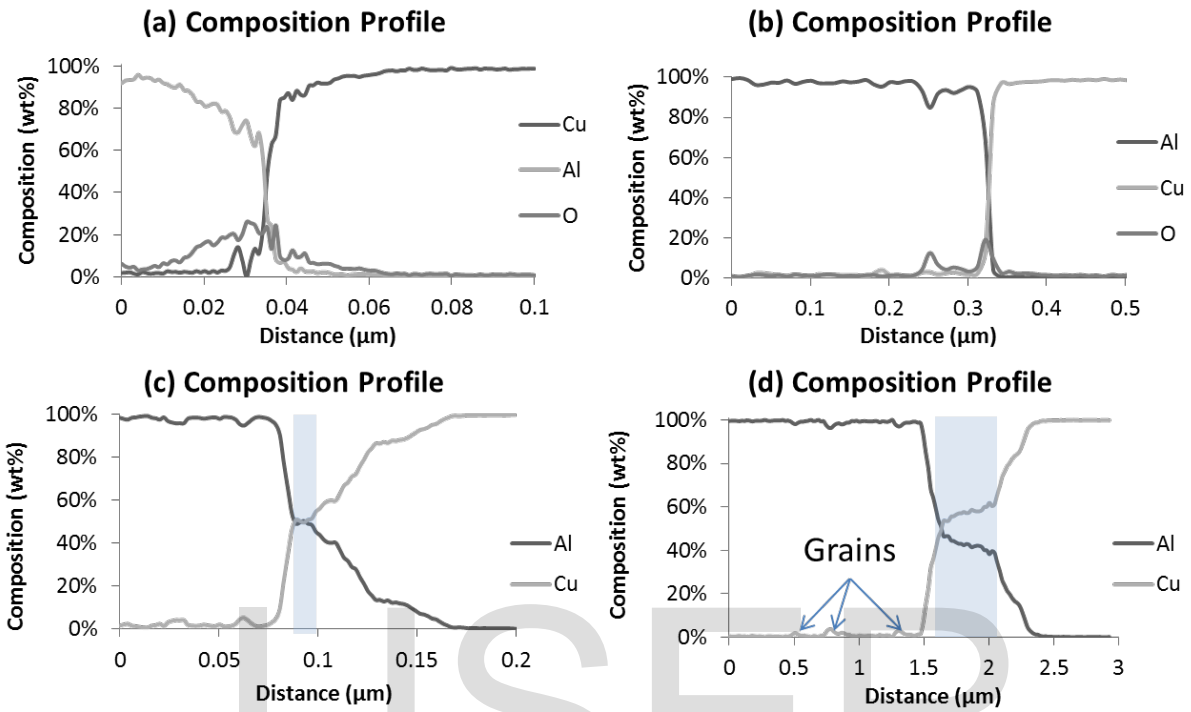

Figure 5

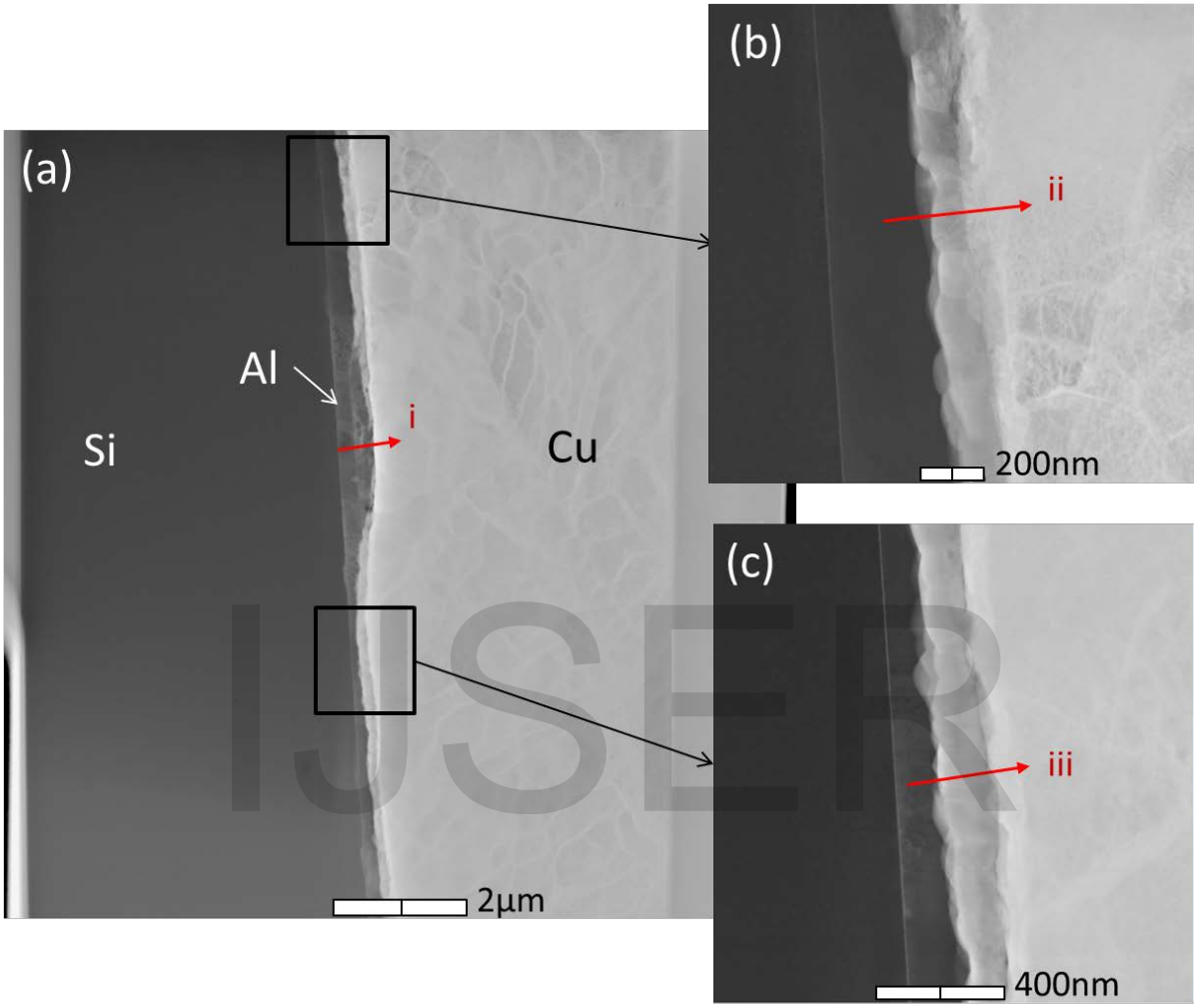

Figure 6

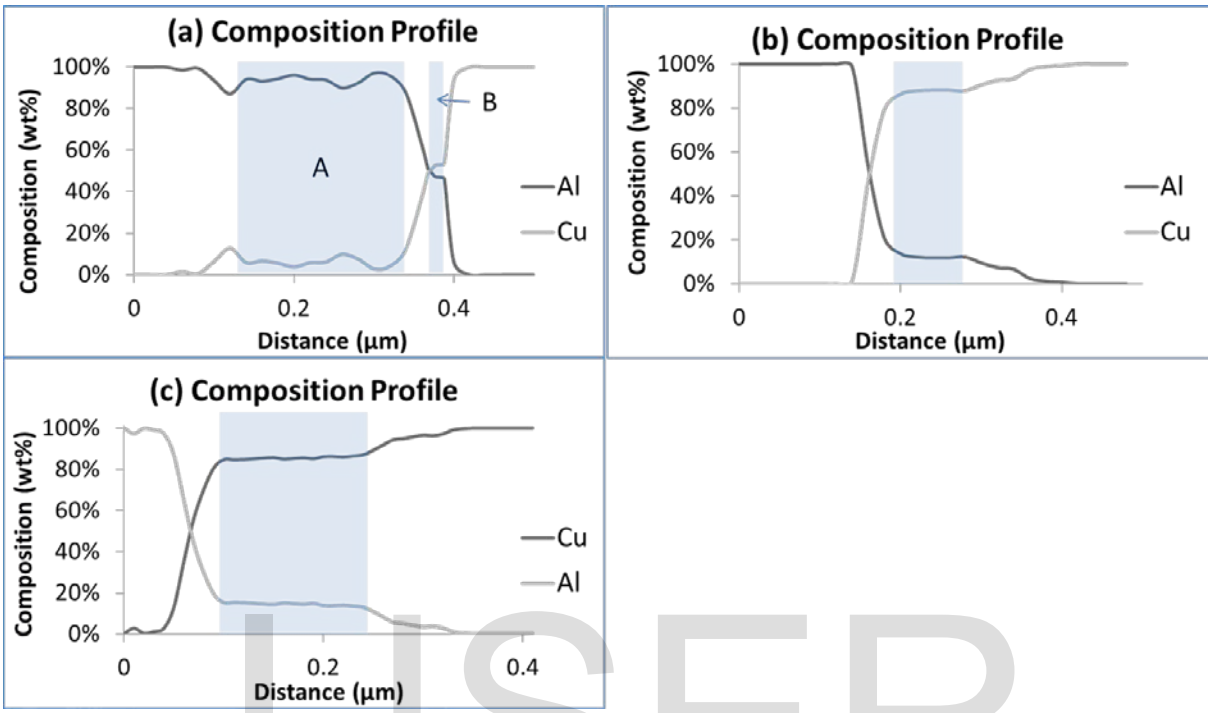

Figure 7

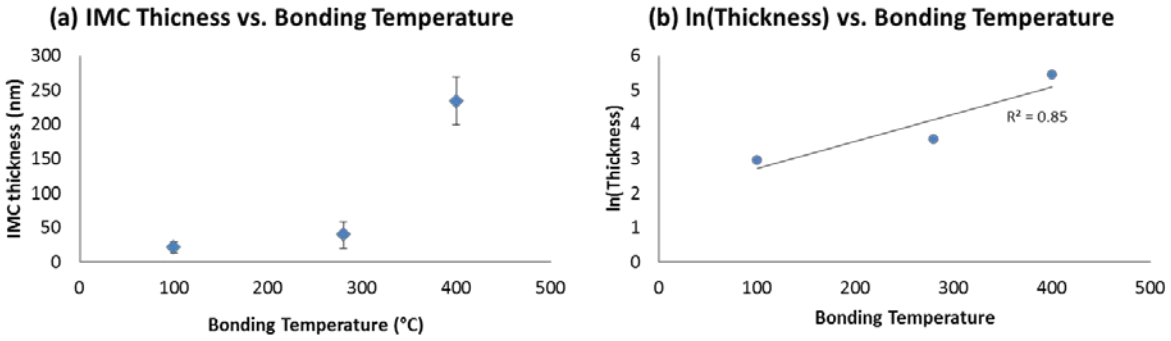

Figure 8

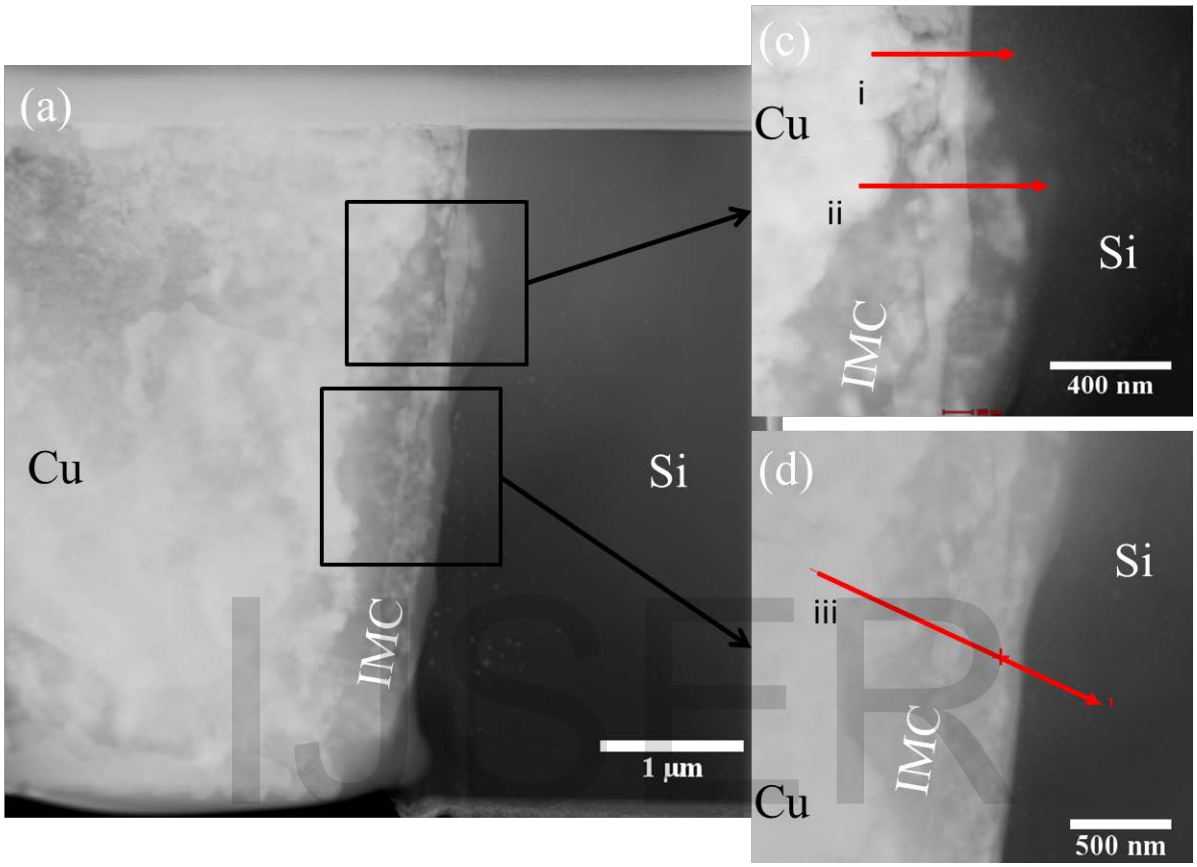

Figure 9

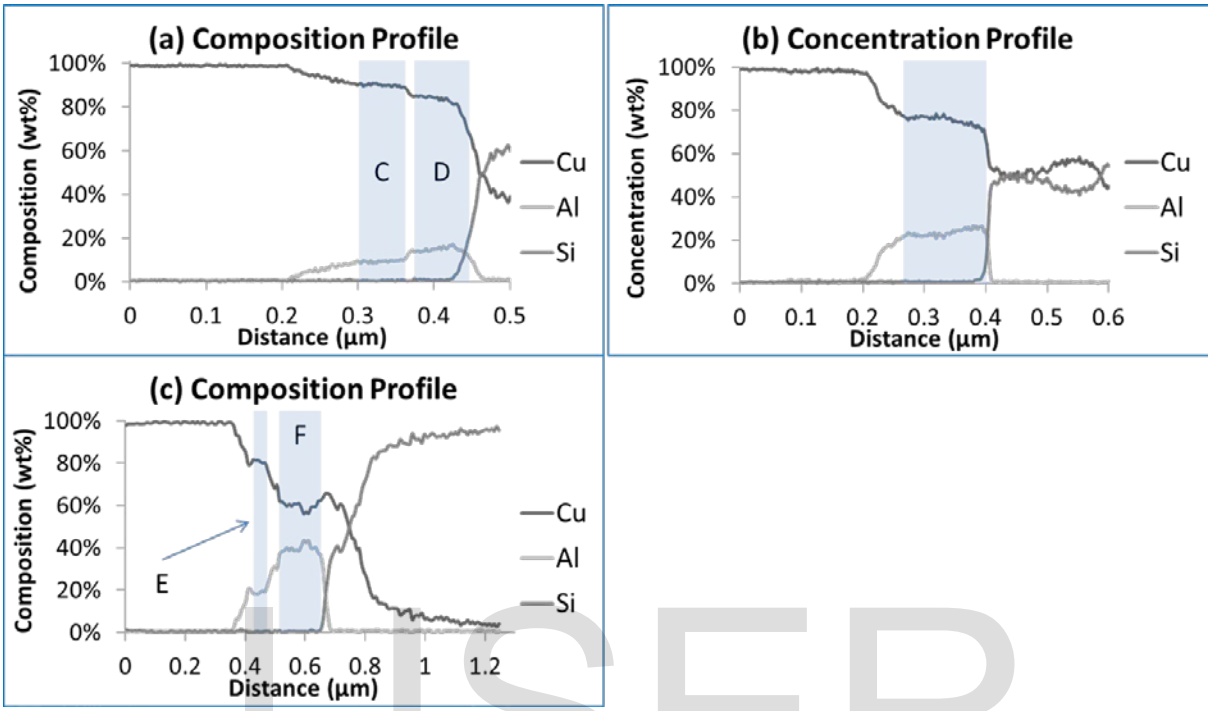

Figure 10

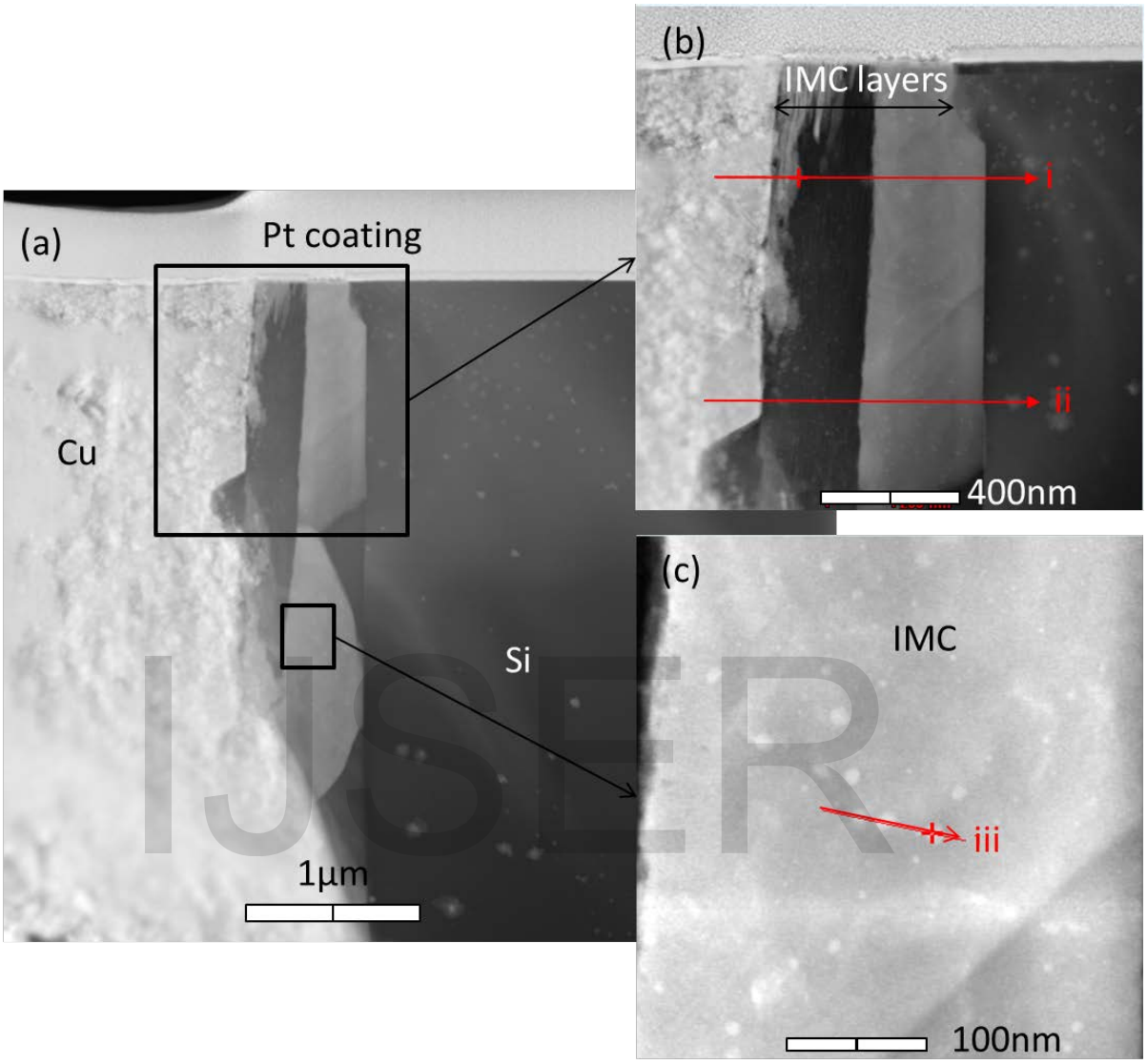

Figure 11